



A Novel AA3105-SiC Composite Fabrication Method

M. Houshyar¹, S. Nourouzi², H. Jamshidi Aval^{2*}

¹Department of Mechanical Engineering, Babol Noshirvani University of Technology, Babol, Iran

²Department of Materials Engineering, Babol Noshirvani University of Technology, Babol, Iran

Review History:

Received: Oct. 20, 2020

Revised: Apr, 03, 2021

Accepted: Apr, 04, 2021

Available Online: Apr, 06, 2021

Keywords:

Aluminium matrix composite

Friction stir processing

SiC particles

Mechanical property

ABSTRACT: Conventional methods of composite production using friction stir processing are simple, rapid, and economical. However, homogenizing the reinforcing particles in the processing zone is very difficult. In addition, this method mainly focuses on surface composite production, while obtaining bulk composites is still challenging. This study investigates the production of AA3105-SiC aluminum matrix composite using the sandwich method as the manufacturing process. The SiC particles were applied through spraying as a layer between AA3105 aluminum sheets. Then, the effect of friction stir processing parameters is investigated. The results indicate an enhanced degree of stirring and plastic deformation following increasing the rotational to translational speed ratio (w/v), which leads to homogenization of the particle distribution in the aluminum matrix. By increasing the w/v ratio, the distribution coefficient decreases from 0.58 to 0.21, which indicates an improvement in the distribution of particles in the matrix. The friction stir processing using the sandwich method significantly improves the mechanical properties of the AA3105-SiC bulk composite compared with the processed samples without reinforcement, with a maximum increase of 192 % in ultimate tensile strength and 273 % in toughness at 1600 rpm and 31.5 mm/min.

1- Introduction

Due to the importance of the net weight of the manufactured parts, the use of lighter metals in today's industry has received much attention. Aluminum and its alloys are among the most important metals used in today's industry due to their high strength-to-weight ratio. In recent years, numerous methods have been proposed and developed to improve the properties of aluminum, the most important of which is the manufacturing of composites. With desirable properties such as high strength, high wear resistance, good fatigue strength, and good strength at high temperatures, composites have become the most important engineering material in the last decade. The high strength-to-weight ratio and wear resistance of aluminum-based composites have received much attention in the aerospace and automotive industries in the last three decades. Highly used reinforcements, including Al_2O_3 , SiC, B_4C , AlN, and Gr. Metal matrix composites are produced using different methods and are selected according to the desired properties and available facilities. These methods are divided into three general categories, namely solid, liquid, and gas. Physical vapor deposition is one of the most prominent methods of production of composites in the gas state. Thermal evaporation is a process that takes place in a vacuum environment. In this process, the source material is evaporated with the help of an electric arc, plasma torch,

or laser beam. The evaporation ratio of the evaporated material to the substrate in this process is in accordance with the pressure difference between the source material and the substrate. The disadvantages of this method include high energy consumption, high temperature, and formation of adverse chemical reactions between the matrix and the reinforcement. Stir casting is one of the simplest and least expensive methods for the production of metal matrix composites in the liquid state, where the reinforcing powder particles are added to the melt and stirred. In this method, the volume fraction of the reinforcing particles is usually less than 30%. The disadvantages of this method include non-uniform distribution and local accumulation of particles in the matrix, which is performed to improve distribution in semi-solid conditions. In the powder metallurgy method, also known as the solid-state method, a mixture of reinforcing particles and matrix powder is initially prepared and pressurized. Then, the mixture is subjected to de-gasification operation for a certain period of time. Next, to eliminate porosity, isostatic axial pressure is applied at high temperatures. Finally, to eliminate porosity and improve the microstructure, the piece is usually subjected to processes such as extrusion [1].

Friction Stir Processing (FSP) is a solid-state method, highly considered in the literature in recent years. The FSP is based on Friction Stir Welding (FSW), which was invented by TWI Ltd in 1991 as a solid-state joining method, and was initially employed for aluminum alloys. The basic concept

*Corresponding author's email: h.jamshidi@nit.ac.ir



of FSP is very simple. In this process, a non-consumable rotating tool is employed with a specifically-designed pin. After inserting the tool into the sheet or plate, it moves along the processing line. During FSP, heat is produced near the contact surface of the shoulder and pin, which varies depending on the geometry of the workpiece. In this process, the material is exposed to a combination of severe plastic deformation and high local temperatures. As a result, the grains become fine and equiaxed. The mechanism of heat generation in FSP is dependent on the process parameters, the thermal conductivity of the workpiece, the geometry of the tool, the shape of the pin, and the material of the backing plate [2]. The FSP falls into the category of hot working processes, where the working temperature reaches the recrystallization temperature of the processed materials. Severe plastic deformation and an increase in temperature due to friction provide the necessary conditions for recrystallization. To achieve the best properties in samples produced using FSP, tool geometry and process parameters, such as translational and rotational speed, must be optimized.

In particle-reinforced composites, the size of the particle plays a crucial role in the properties of the composite. Very fine (nanometer) particles with proper distribution in the matrix prevent dislocations and increase the strength of the material. Strengthening using particle reinforcement is similar to precipitation hardening. Compared to precipitates that dissolve at high temperatures, secondary phase particles distributed in ceramic-reinforced particle composites are often stable at high temperatures, and therefore, retain strength. Hard particles in the soft matrix (such as ceramic particles in the metal matrix) increase the resistance to wear. Moreover, large particles transfer the applied force to the base alloy (matrix), which leads to an increase in strength [3]. So far, the FSP method has been used to manufacture a variety of aluminum and magnesium matrix composites, with added reinforced particles including SiO_2 , carbon nanotubes, Al_2O_3 , and SiC. The use of SiC as reinforcement in aluminum matrix composites is desirable in particular since it increases strength, wear resistance, and thermal stability [4]. The density of SiC (3.2 g/cm^3) is close to aluminum (2.7 g/cm^3). Therefore, its high resistance to acids, alkali, and molten salt (up to approximately $800 \text{ }^\circ\text{C}$) yields a suitable reinforcing material in aluminum matrix composites to produce strong materials with excellent mechanical properties [5]. Composite production by FSP is divided into direct and indirect groups. In the direct method, particles are initially placed on the surface using different methods (grooving or drilling on the surface). Then, the FSP is processed so that the particles are placed directly on the matrix. In the indirect method, the reinforcing particles are first mixed with the base metal powder. Then, they are pressed using a hot- or cold-press process, and finally, the final composite is produced using FSP [6].

Producing Al-SiC surface composite using the FSP method was first reported in Mishra et al. [7]. In this study, SiC powder was applied as a layer over the surface of AA5083 using methanol, and the surface was dried afterward. This method has been used in other studies to apply powder in the

process [8, 9] with similar results. However, these methods have limitations in enclosing the powder and the depth of penetration of the powders. Therefore, other methods, such as drilling and grooving on the surface, were utilized. These methods have been extensively employed in research and yielded better results compared with the previous methods. Sahraeinejad et al. [10] examined the effect of different particles on the mechanical properties of composites. They reported that the slope of the hardness-volume fraction diagram for 20 nm SiC and Al_2O_3 particles is more than Al_2O_3 particles with $1.1 \mu\text{m}$ and $4.3 \mu\text{m}$ sizes. Moreover, this study reported an increase in hardness from 110 to 162 VHN with a slight increase in SiC volume fraction. It should be noted that the use of SiC in the aluminum matrix leads to the formation of very fine grains because these particles have significant effects on locking dislocations. Devaraju et al. [11] observed that the wear rate in AA6061/ SiC- Al_2O_3 composite was lower in 8vol.% SiC and 2 vol.% Al_2O_3 due to the uniform distribution of the particles. There is a significant decrease in the composite wear rate in the AA8026 matrix, where Al_2O_3 and TiB_2 particles are uniformly distributed in the matrix [12]. However, with the increase in the partial volume fraction of reinforcements in AA6061 / SiC- Al_2O_3 composite, its wear performance weakened, which is related to the particle clustering in the matrix. Mahmoud et al. [13] observed that in a composite containing 20% Al_2O_3 and 80% SiC, the detached Al_2O_3 particles form a thin layer on the worn surface, which acts as a protective layer that reduces the coefficient of friction and the wear rate. Mohamadigangaraj et al. [14] investigated the effect of FSP parameters on microstructure and mechanical properties of A390- 10 wt.% SiC. They found that the shoulder-to-pin diameter ratio posed the most significant impact on the composite toughness. Raheja et al. [15] studied the development of hybrid Gr/SiC reinforced aluminum matrix composite through friction stir processing. They reported the hardness and strength of 1.75 GPa and 78 MPa, respectively, for hybrid Gr/SiC reinforced aluminum matrix composite. Sharma et al. [16] investigated Al-SiC-GNP composite produced by FSP. They found that the higher strength of Al-SiC-GNP composite was attributed to the mechanical exfoliation of GNPs to few-layered graphene in the presence of SiC. Prabhu et al. [17] investigated the effect of multi-pass FSP on AA6082-SiC composite. They reported that the strong interfacial bonding between the SiC particle and Al matrix after three pass FSP resulted in the high ultimate tensile strength. Jain et al. [18] studied the FSP of AA5083-CNT-SiC composite. They reported that particle stimulated nucleation and Zener-Holloman mechanism were the dominant restoration mechanism in the hybrid aluminum matrix composite.

Although the direct method to fabricate composites using FSP is simple, rapid, and cost-effective, homogenizing the reinforcing particles in the processing zone is very difficult. In addition, this method mainly focuses on surface composite production, while obtaining bulk composites is still challenging. One approach for improving the direct method and enabling the fabrication of bulk composites using

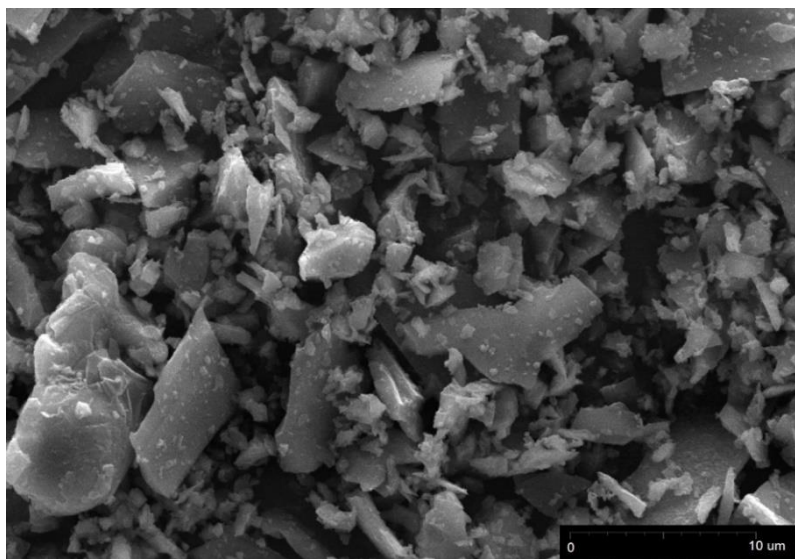


Fig. 1. SEM image of SiC particles.

Table 1. Chemical composition of AA3105 alloy (wt%).

Al	Mg	Si	Fe	Cu	Mn
Balancing	0.26	0.40	0.70	0.10	0.68

FSP is the sandwich method, first proposed by Mertens et al. [19]. This method can apply a high-volume percentage of reinforcements and produce bulk composites. Moreover, common problems encountered in methods that apply the powder using holes and grooves, such as unfilled holes and grooves embedded in the base metal, are eliminated using the sandwich method. It should be noted that the sandwich method has some limitations in applying different weight percentages of the reinforcing material. However, using conventional methods to apply different weight percentages of the reinforcing material requires drilling or grooving on the entire surface of the base material, and since the processing area is only at the tool pin zone, the surface of the material must be drilled or grooved again after each pass. Therefore, since in the sandwich method, the reinforcing material is applied between the sheets and in the initial processing step, it does not require drilling or grooving after each processing step. In this study, the production of the AA3105-SiC metal matrix composite is investigated using the sandwich method, as a novel method for fabricating bulk composites. The SiC particles, with the range of sizes 1-20 μm , are applied as a layer between the sheets. Then, the effect of rotational and translational speeds on the distribution of reinforcement particles and the mechanical properties of the composite are evaluated.

2- Experimental Procedure

In this study, AA3105 aluminum sheets, with thicknesses of 1 and 2 mm, are used as the composite matrix. The chemical composition of these materials is demonstrated in Table 1. Moreover, in this study, SiC powder, a range of particle sizes between 1-20 μm , is used as the reinforcing particle. Fig. 1 demonstrates the Scanning Electron Microscopy (SEM) image of the SiC powders. The aluminum was cut in 10 \times 15 cm^2 sheets. Then, four holes are drilled in the corners of these sheets for riveting them in before the FSP step. Next, a wire brush was utilized to remove contaminants and scratches, so that the SiC powders can settle on the surface. The reinforcing particles were then suspended in ethanol and sprayed over the outer surfaces of the sheets. After a few hours, the alcohol is evaporated from the surface of the sheet, while the powders remain. For each FSP sample, four sheets were employed. In specific, 2 mm sheets were placed over the top and bottom, and 1 mm thick sheets were placed between them. Finally, these 4 sheets are pressed, and the 4 corners of the previously perforated sheets are riveted. The steps for preparing FSP samples are presented in Fig. 2. FSP was performed on the sheets using the FSP machine in position control conditions. A threaded cylindrical tool constructed by high-speed steel is used for FSP. The diameters of the shoulder and pin are 18 and 6 mm, respectively, while the height of the pin is 5.7

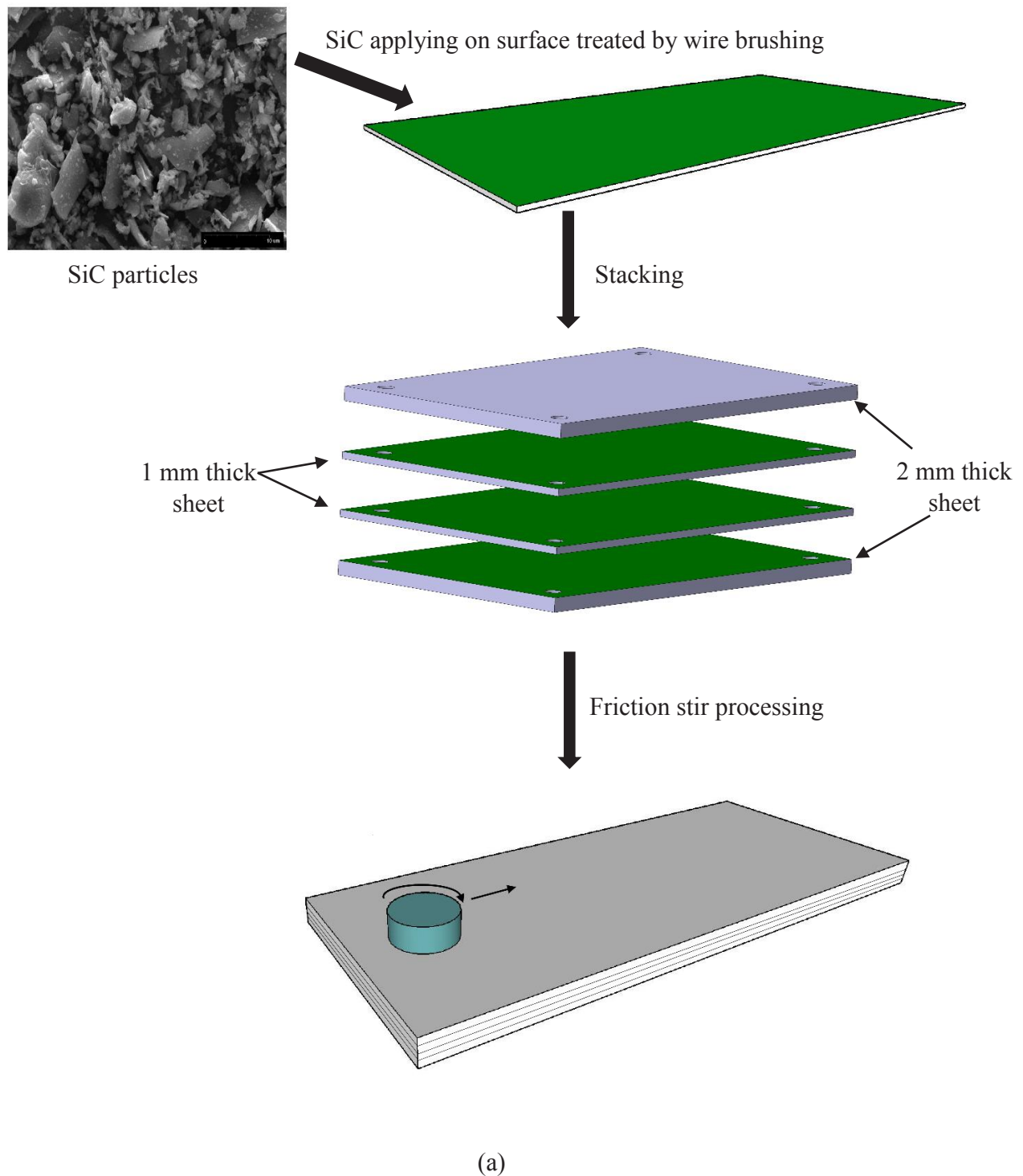


Fig. 2. a) Schematic illustration of the sandwich method for fabrication of Al-SiC composite via FSP, b) AA3105 sheet after each step of sample preparation.(Continue)



AA3105 sheet after surface preparing by wire brushing



AA3105 sheet after spraying SiC particles



Prepared sample before FSP and after stacking and riveting



Sample after FSP

(b)

Fig. 2. a) Schematic illustration of the sandwich method for fabrication of Al-SiC composite via FSP, b) AA3105 sheet after each step of sample preparation.

Table 2. Friction stir process designation.

Sample No.	Rotational speed (rpm)	Translational speed (mm/min)
1	1250	31.5
2	1250	40
3	1600	31.5
4	1600	40

**Fig. 3. FSP tool used in this study.**

mm. This tool is illustrated in Fig. 3. The tool shoulder is concave with a 2° conical cavity. The process was performed in four passes with four rotational speeds (500, 800, 1250, and 1600 rpm) and two linear speeds of 31.5 and 40 mm / min. According to preliminary studies, mixing the reinforcing particles at high rotational speeds (1250 rpm and 1600 rpm) is considerably better than lower rotational speeds. Also, at rotational speeds higher than 1600 rpm and transitional speeds lower than 31.5 mm/min due to excessive heat input, a tunnel defect was observed in the composite. FSP with a transitional speed higher than 40 mm/min results in tunnel defect in the processing zone. Therefore, subsequent studies are performed on FSPed samples at rotational speeds of 1250 and 1600 rpm and transitional speeds of 31.5 and 40 mm/min. It should be noted that the rotation direction of the tool (clockwise or counterclockwise) is changed after each pass. Table 2 shows the design of experiments of samples.

After the FSP, all samples were cut for metallurgical examination. After grinding by 160-3000 grit sandpapers and polishing with 1 μm alumina suspension, the microstructure of all samples was evaluated using optical microscopy (DG Victory-Dewinter) and FEI ESEM QUANTA 200 scanning electron microscope equipped with X-ray diffraction (EDS). The distribution of the particles in the aluminum matrix, along

with the morphology and size of the particles, was evaluated by microscopic observations and image analysis with Clemex software. The Distribution Factor (DF) is calculated by dividing the particle surface standard deviation on its mean particle surface fraction [20]. After preparing the cross-section of the FSPed samples, the hardness of the both composite and the AA3105 base metal were investigated by Vickers micro hardness test using a load of 100 gf for 15s on Koopa microhardness tester MH4. The tensile test samples were prepared in accordance with ASTM E8M in the longitudinal direction and from the processing zone. The tensile test was performed using a SANTAM-250 Universal Testing Machine at room temperature and a constant crosshead speed of 1 mm/min with three repeat times. The tensile toughness is calculated by using the area underneath the stress–strain curve. The Origin 9 software was used to calculate the area underneath the stress–strain curve.

3- Results and Discussion

3- 1- Macrostructure and microstructure of the composites

Figs. 4 and 5 demonstrate the macroscopic image from the top surface and the cross-section of the FSPed samples. The effective parameters in the material flow in the stir zone must be considered to provide suitable mixing in the

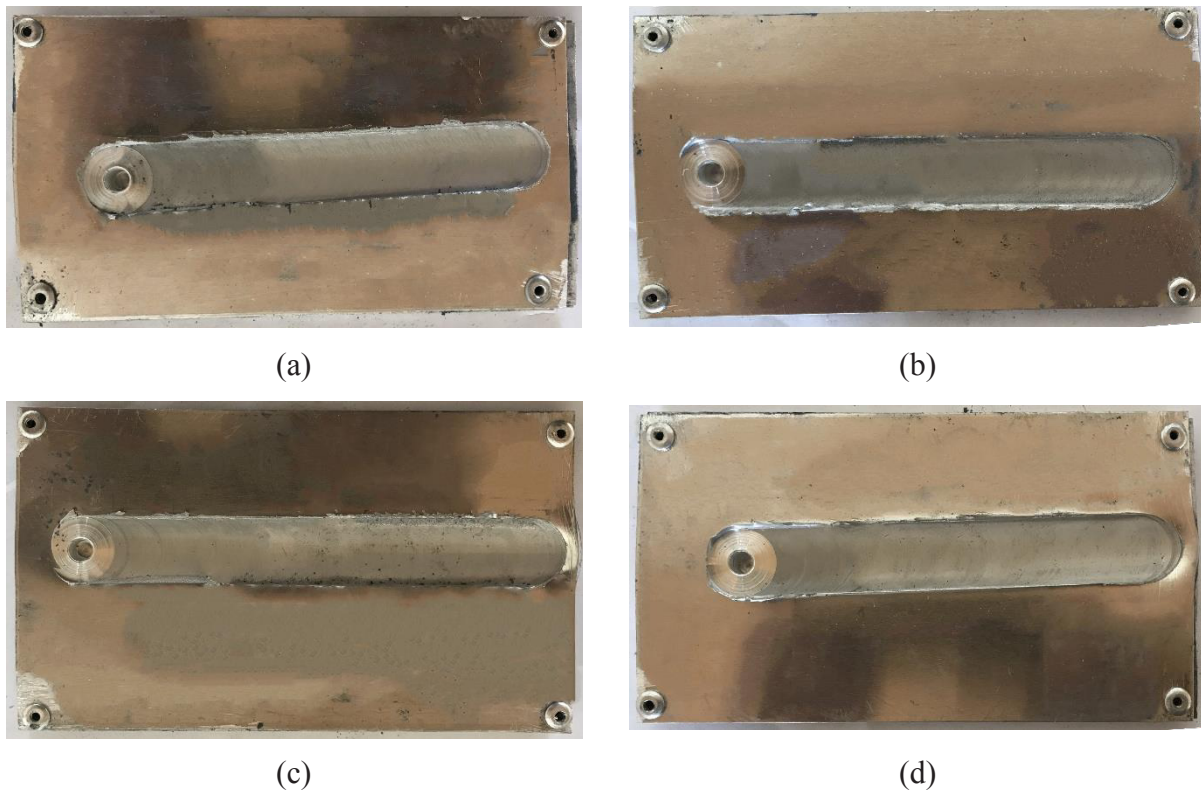
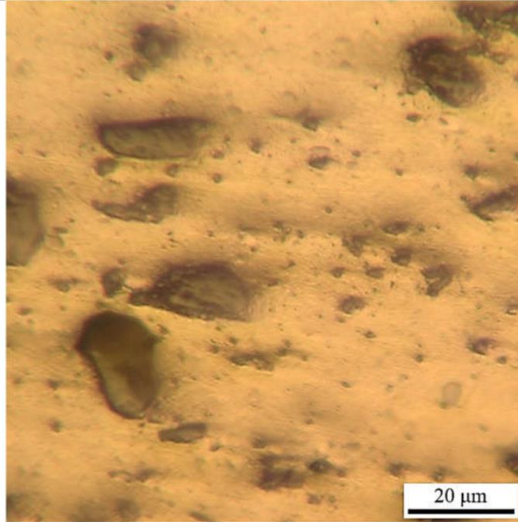
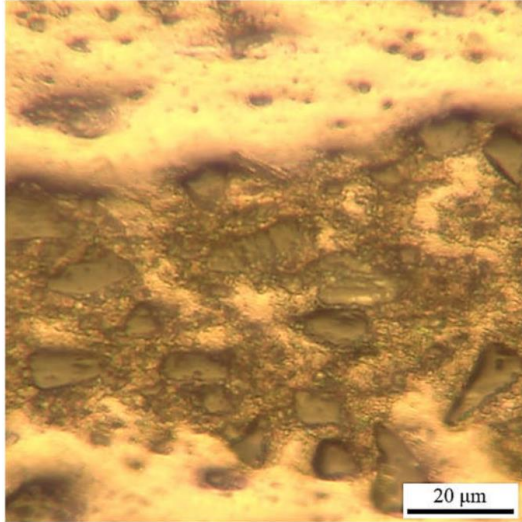
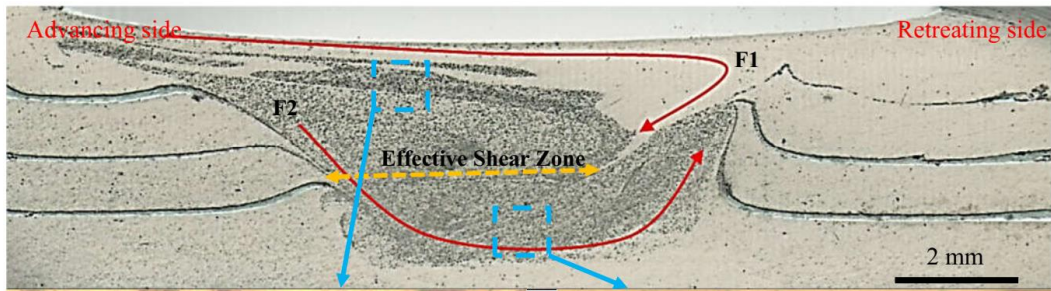


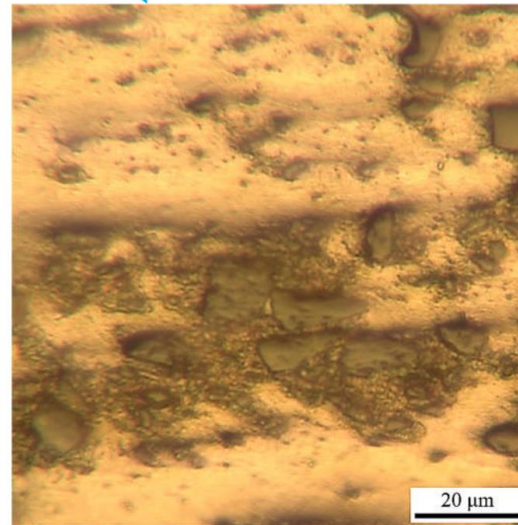
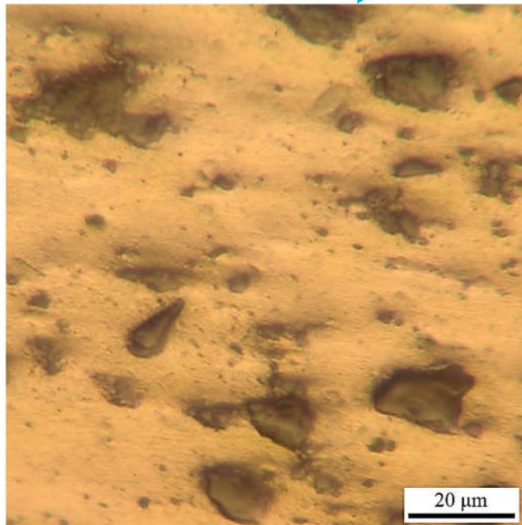
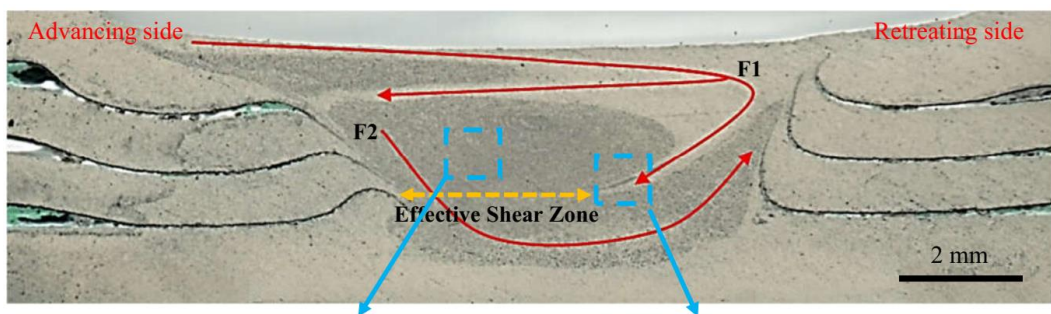
Fig. 4. The top surface of friction stir processed samples; a) sample no.1, b) sample no.2, c) sample no.3, d) sample no.4.

stir zone. One of the important parameters is the ratio of rotational speed to translational speed (rotational speed w , translational speed v). It should be noted that at very low rotational speeds, the materials cannot properly flow, and tunnel-like defects are created along the processing zone [21, 22]. In fact, the presence of tunnels or cavities in different areas of the stir zone is attributed to the heat input during the FSP. Based on Ref. [23], the ratio of rotational speed to the translational speed of the tool is assumed as a criterion of heat input per unit length of friction stirred samples—the heat input increases by increasing the rotational speed. High heat input causes the easier flow of material around the pin and raises the possibility of flash forming. Furthermore, excessive heat input increases the likelihood of cavities or tunnels, mainly due to loss of material support at the trailing side of the tool [24-26]. The sound cross section of FSPed samples at different rotational speeds indicates that the heat generated during FSP is sufficient for the process. In the cross-section, the reinforcement particles can be seen in dark colors. As can be seen, the size of SiC particles is reduced significantly. Previous studies [27-29] pointed out that due to the thermomechanical nature of FSP, which is a combination of frictional heat and plastic deformation, it is possible to fracture reinforcement particles. Therefore, as the rotational speed increases, the particles in the matrix are distributed more homogeneously. On the other hand, microscopic studies

confirm that the number of particles at the top of the stir zone is less than those at the bottom. This phenomenon is specifically noticeable at lower rotational speeds. At high rotational speeds, the higher temperature near the tool shoulder, and the force applied by the tool shoulder in the upper area (the shoulder affected zone), contribute to greater uniformity of the stir zone. According to the images, the macrostructure of the samples and the distribution of SiC particles are different. In addition, it can be concluded that the process parameters, especially rotational speed, have significant effects on particle distribution and grain size [30, 31]. In the upper area of the stir zone, in the sample with lower heat input (sample no. 2), a powder-free zone was observed, which in comparison with the sample with higher input heat (sample no.3), had a relatively less uniform distribution. Thus, the results confirm the positive effect of increasing the heat input on the particle distribution in the matrix. In other words, by increasing the heat input, a more homogeneous structure will be obtained. In this process, severe deformations, along with a high w/v ratio, results in uniform distribution [32]. It should be noted that kissing bond defects are visible in almost all samples. As shown in Fig. 5 (a), material at the top layer of the stir zone that flows from the advancing side to the retreating side (shown by F1) forms a reinforcing particles-free layer. At the bottom of the stir zone, a different flow is formed that flows the reinforcing particles from the advancing side to the



(a)



(b)

Fig. 5. Macroscopic and microscopic photographs of the friction stir processed samples; a) sample no.1, b) sample no.2, c) sample no.3, d) sample no.4. (Continue)

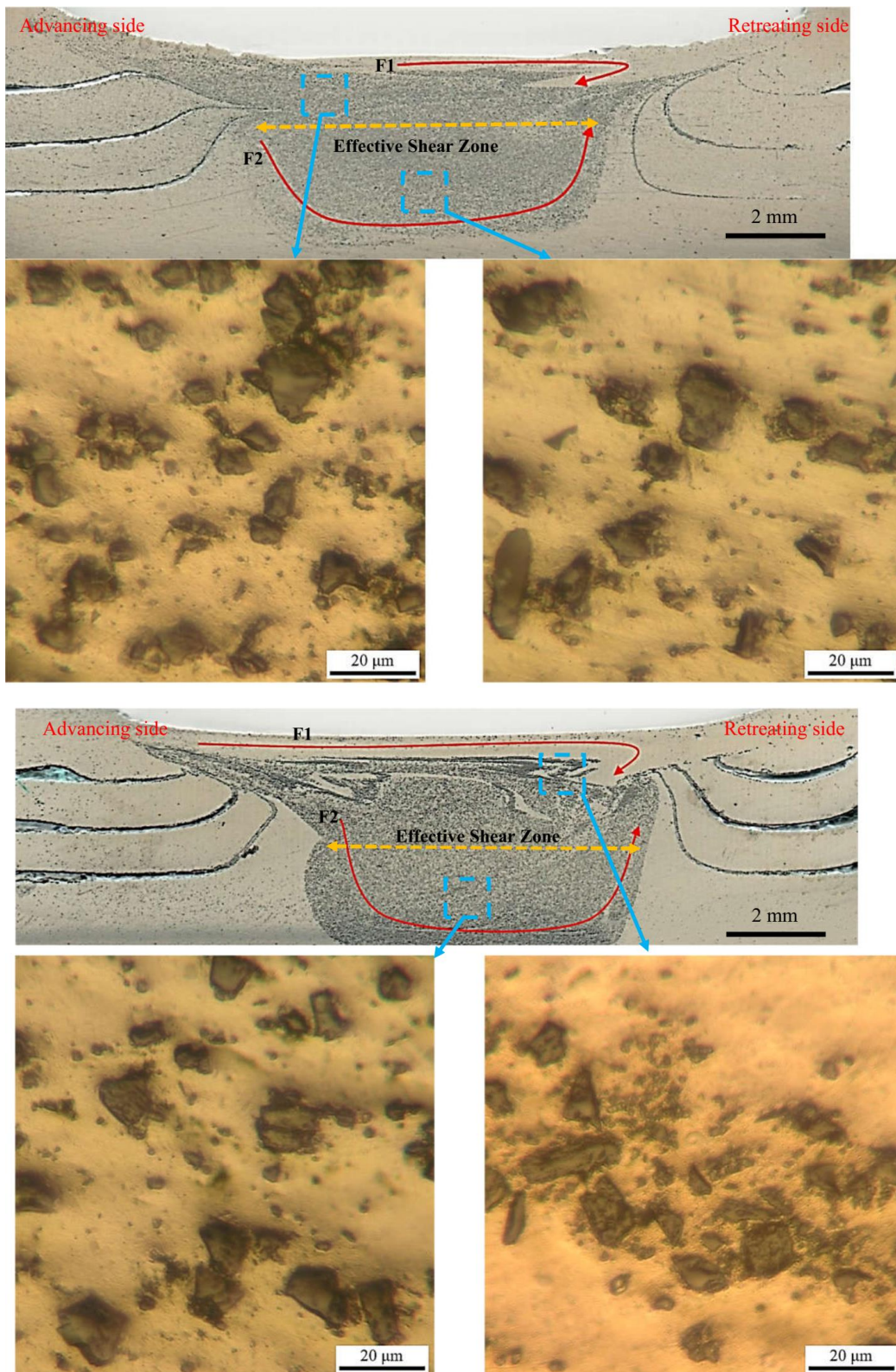


Fig. 5. Macroscopic and microscopic photographs of the friction stir processed samples; a) sample no.1, b) sample no.2, c) sample no.3, d) sample no.4.

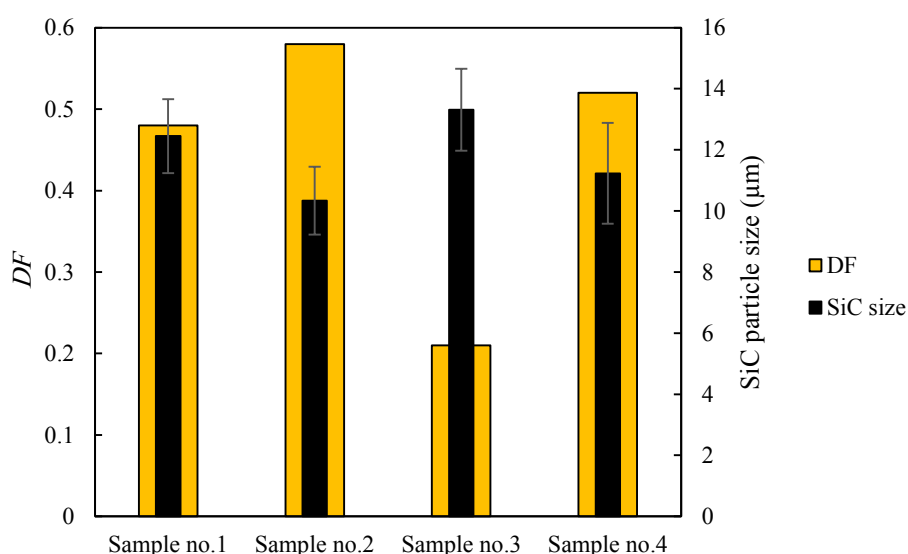


Fig. 6. Variation of DF and SiC particles size in the stir zone of different samples.

retreating side (shown by F2). The interaction of flows F1 and F2 yields the formation of onion rings in the stir zone (this circular structure is visible more clearly at low heat inputs). As the heat input increases, the effect of the pin on the material flow increases, and the material flow induced by pin (F2) becomes stronger than the material flow generated by the shoulder (F1). There is also an effective shear zone on the advancing side with no trace of clustering and accumulation of reinforcement and uniform distribution. It is noteworthy that with the increase of heat input, the effective shear zone increases. According to the microscopic images provided in Fig. 5, no defect was observed in the accumulation zone. According to the images, in the maximum heat input in the Effective Shear Zone (ESZ), a proper process zone and uniform distribution of particles are observed. As can be seen, with the increase of heat input, the SiC particles are less broken, and a more homogeneous structure can be created.

The DF and the average size of SiC particles for the FSPed samples are shown in Fig. 6. As can be seen, decreasing the heat input results in a decrease in the size of the SiC particles. However, as the heat input increases, the distribution coefficient decreases from 0.58 to 0.21, indicating an improvement in the distribution of particles in the matrix. The effect of heat input on the size of the particle in the stir zone can be explained by the fact that when the heat input is reduced, the flow stress in the processing zone is much higher than in the conditions where the heat input is maximum. As a result, reducing the heat input forms bigger stress at the interface of matrix and reinforcement and increasing the probability of particle fragmentation. However, lower flow stress in the matrix decreases the stress on the interface of particles and the matrix. Therefore, particles are not sufficiently fragmented by interfacial stress. In these

conditions, due to lower flow stress in the matrix, particles will move with the matrix. Therefore, due to severe plastic deformation and a higher degree of the material mixture in the sample with maximum heat input, uniform distribution of the reinforcing particles and a decrease in the distribution coefficient are expected. The effect of increasing the heat input on enhancing the uniformity in the reinforcing particle distribution during FSP is reported by other researchers [33].

3- 2- Hardness and strength of composites

Mechanical properties of aluminum matrix composites in FSP are generally dependent on the presence of macro defects in the stir zone, plastic deformation, martial mixing, grain size, distribution, and size of the reinforcing particles. Various strengthening mechanisms improve mechanical properties in composites reinforced with SiC, including the transfer of load from the matrix to reinforcing particles [34, 35]. Another strengthening mechanism is a result of microstructure changes of the composite [36]. The first mechanism in this section involves grain refining according to the Hall-Patch equation, which increases the strength. In the second mechanism, the uniform distribution of reinforcing particles, along with an increase in their number due to fracture of particles, restricts dislocations movement, which increases the stress required to move dislocations. The interface bonding between reinforcing particles and the matrix transfers the stress from the matrix to reinforcing particles and increases the strength, which is considered as the third mechanism. Finally, in the fourth mechanism, the large thermal expansion coefficient difference between the matrix and SiC particles leads to an increase and accumulation of dislocations near the interface, preventing the free movement of dislocations [37]. Fig. 7 shows the interface between particles and the matrix in

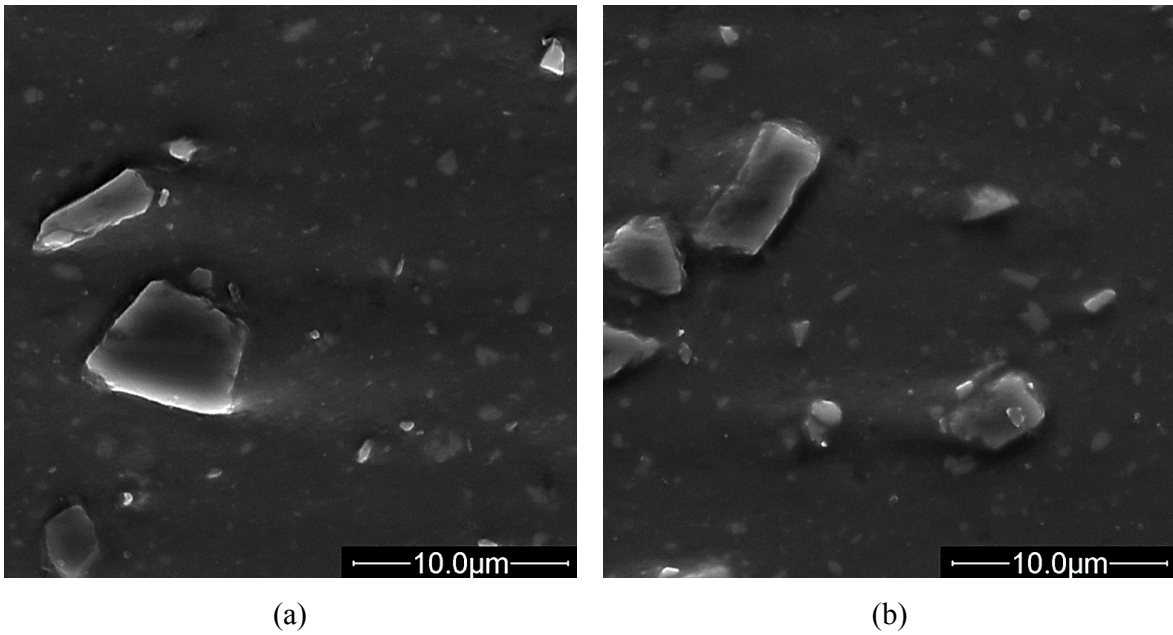


Fig. 7. SEM image of; a) stir zone of sample no.2, b) stir zone of sample no.3.

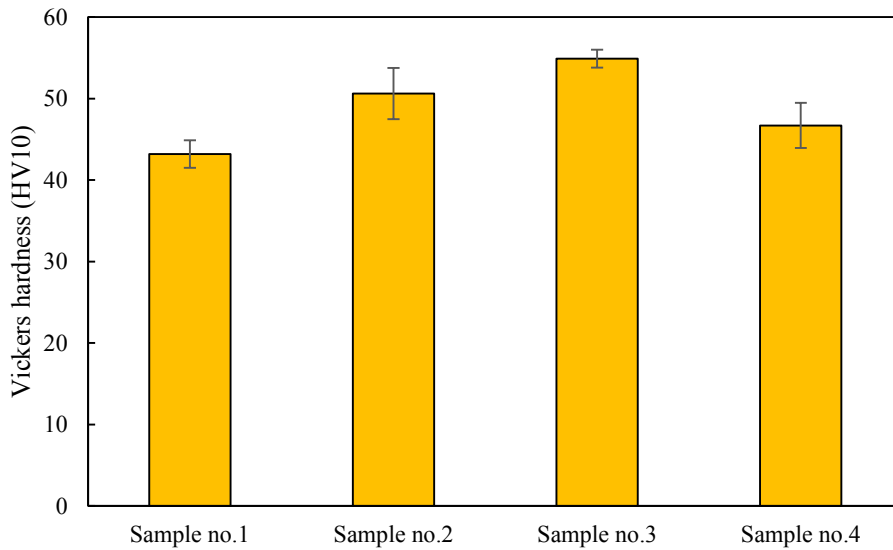
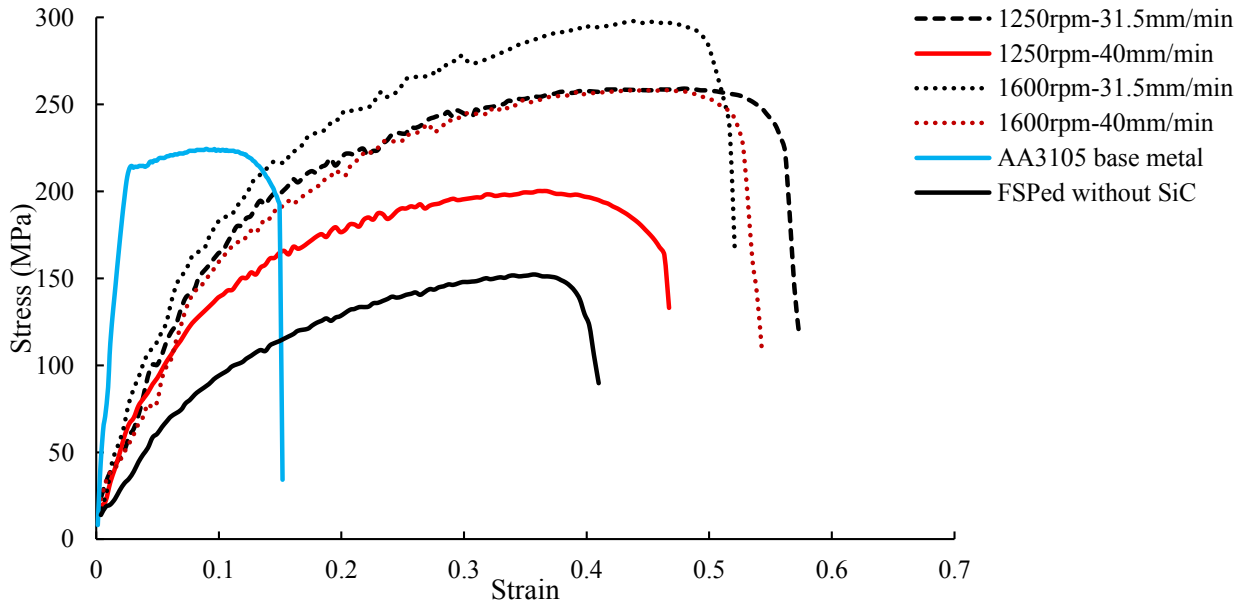


Fig. 8. Variation of stir zone hardness.

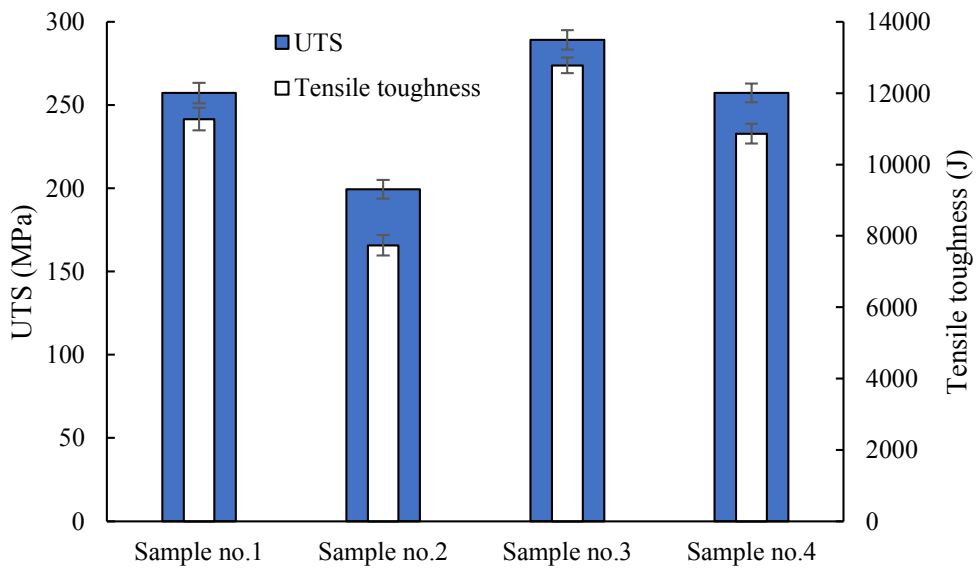
samples with the lowest and highest heat inputs. As can be seen, the interface is fully integrated, indicating a proper bonding between particles and the matrix. Moreover, the effect of rotational and translational speed on the average hardness of the stir zone is demonstrated in Fig. 8. It should be noted that the hardness deviation was more in samples with lower heat input than in other samples, which could be due to the fact that in samples with lower heat input, larger

particle aggregation regions form in the stir zone. Therefore, these zones can yield unexpected higher hardness and bigger hardness deviation in the stir zone.

The tensile strength and the toughness of the AA3105-SiC composites are shown in Fig. 9. As can be seen, both indices increased with increasing heat input. The composite toughness was 11.275 ± 0.004 , 7.734 ± 0.003 , 12.778 ± 0.002 , and 10.863 ± 0.002 kJ at w/v ratios of 39.68, 31.25, 50.79,



(a)



(b)

Fig. 9. a) The stress-strain curve, b) Variation of stir zone UTS, and tensile toughness of different samples.

and 40 rev/mm, respectively. By increasing the heat input, the toughness of the composite increased 377%, 258%, 427%, and 363%, respectively, compared with the AA3105 base metal (2.901±0.003 kJ). Also, increasing the heat input increased the tensile strength of the composite, compared with the FSPed sample without reinforcing the particles. The tensile strength of the composite was 257.21±6.20, 199.46±5.66, 289.21±5.80, and 257.27±5.61 MPa at w/v ratios of 39.68, 31.25, 50.79, and 40 rev/mm, respectively. By increasing the heat input, the composite toughness experienced an increase of 171%, 133%, 192%, and 171%, respectively, in comparison with the FSPed sample with maximum heat input and no reinforcing particles (150.22±6.21 MPa) (this sample labeled as “FSPed without SiC” in Fig. 9 (a)). Although other researchers didn't study a similar topic, Ahmadifard et al. [38] reported that hardness and Ultimate Tensile Strength (UTS) of AA5083-SiC FSPed composite increase 38% and 11% compared to AA5083 base metal. Besides, Kraiklang et al. [39] reported that the UTS of AA5052-SiC FSPed composite increases 14% compared to AA5052 base metal. This simultaneous increase in strength and toughness of the FSPed samples was due to the increased uniformity of the microstructure. The accumulation of SiC particles results in crack nucleation and growth, which is one of the most important factors influencing the tensile behavior of the composite. According to the observations reported in Barmouz et al. [30], the inhomogeneous distribution of SiC particles in the matrix stimulates crack nucleation and growth. The increase in strength in metal-matrix composites depends on proper bonding between the particles and the matrix to which the applied load is transferred. Also, low discontinuity in the interface increases strength [40]. The strength and toughness of sample no. 3 with a rotational to transitional speed ratio of 50.79 revs/mm has the best conditions among other samples to achieve the maximum uniformity.

The SEM images obtained from the fracture surfaces of AA3105, the FSPed samples without reinforcing particles, and the FSPed AA3105-SiC composites with minimum and maximum heat inputs are shown in Fig. 10. The dimples at the fracture surface of the base metal and the processed sample without reinforcing particles (Fig. 10 a, b) indicate a completely ductile fracture in these samples. The fracture mechanism in the processed samples with reinforcing particles follows the cellular fracture mechanism, which occurs in polycrystalline materials. In specific, in cases where the constituent components of the microstructure have different mechanical properties, the cracks formed in each phase are proportional to the characteristics and mechanisms of the failure related to that phase. If the material is brittle, then the brittle fracture mechanism is proposed, and for the soft parts of the material, the ductile fracture mechanism is proposed. This mechanism is shown with white circles in Fig. 10 (c) and (d), which, according to the fracture mechanism, SiC

particles are present within the deformed aluminum grains. An important point in these images is the excellent bonding between matrix and reinforcement. As shown with a red arrow in the image, fracture occurred inside the SiC particles, and no separation in the interface is seen. As can be seen in the SEM images obtained from the composite samples, as the heat input increases, the size of these microvoids, shown with blue arrows, increases. Larger and deeper dimples, made with the maximum heat input, and an average size of 5 μm at the fracture surface of the composite sample are clearly visible, which is due to the higher heat input compared to other samples and larger elongation in this sample.

Although the study of the effect of rotational and transitional speeds considered in this study on FSPed samples showed that the sandwich method can be introduced as a method of manufacturing aluminum matrix composites, it should be considered that for verifying the industrial feasibility and practicality purposes of this composite manufacturing method the other parameters such as the number of layers, the thickness of plates, thickness of sprayed particles should be investigated.

4- Conclusions

In this study, a sandwich method was utilized to manufacture AA3105-SiC aluminum matrix composites via friction stir processing. The microstructure and the mechanical properties of FSPed samples were examined. Based on the experimental results, the main conclusions are as follows:

The distribution of SiC particles in the stir zone is significantly dependent on the level of refinement and the rotational speed of the tool. By increasing the rotational speed and heat input, the material flow induced by the pin will increase, which will result in more uniformity in the stir zone. The maximum uniformity in the stir zone was achieved at rotational speed 1600 rpm and translational speed 31.5 mm/min.

Agglomeration of SiC particles and formation of reinforcing particles free zone at the stir zone for the low-heat input samples result in a bigger deviation in hardness at the stir zone.

FSP on the sandwiched AA3105-SiC aluminum matrix composite can significantly increase the mechanical properties of the AA3105-SiC bulk composite, compared with the processed samples without reinforcement, with a maximum increase of 192 % in UTS and 273% in toughness at 1600 rpm and 31.5 mm/min.

The fracture mechanism in friction processed samples containing SiC reinforcing particles follows the cellular fracture mechanism.

The sandwich method can be used as a simple and rapid method for producing bulk aluminum matrix composite production using FSP.

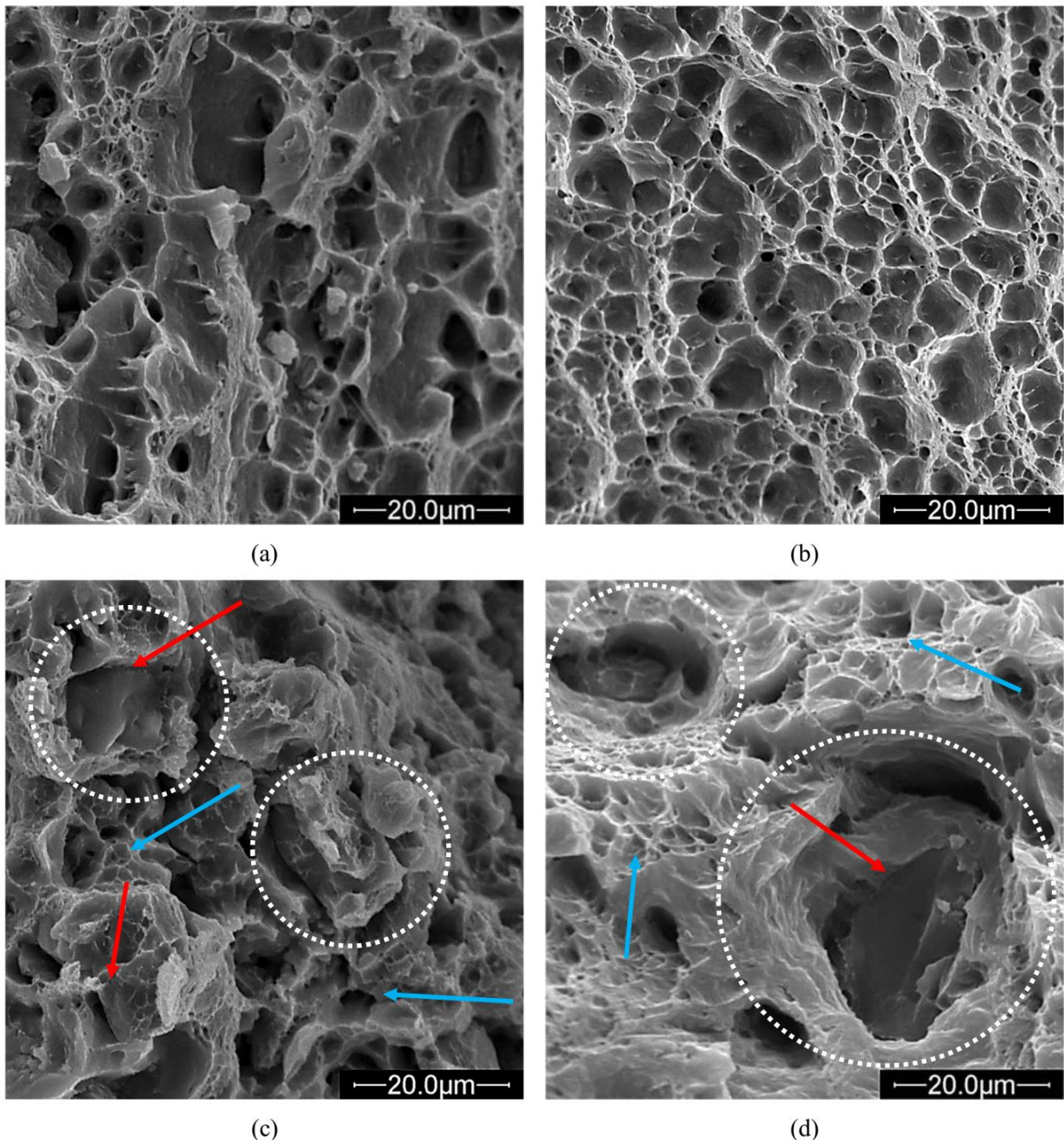


Fig. 10. SEM fractographs of a) base metal, b) FSPed sample without SiC particle, c) sample no.2, and d) sample no.3.

References

- [1] V. Sharma, U. Prakash, B.M. Kumar, Surface composites by friction stir processing: A review, *Journal of Materials Processing Technology*, 224(1) (2015) 117-134.
- [2] H.J. Aval, S. Serajzadeh, A. Kokabi, The influence of tool geometry on the thermo-mechanical and microstructural behaviour in friction stir welding of AA5086, *Proceedings of the institution of mechanical engineers, part c: journal of mechanical engineering science*, 225(1) (2011) 1-16.
- [3] T. Clyne, P. Withers, *An introduction to metal matrix composites*, Cambridge university press, 1995.
- [4] M.M. Moradi, H.J. Aval, R. Jamaati, S. Amir Khanlou, S. Ji, Effect of SiC nanoparticles on the microstructure and texture of friction stir welded AA2024/AA6061, *Materials Characterization*, 152 (2019) 169-179.
- [5] S. Gajalakshmi, K. Sriram, Investigation of mechanical behavior of ultra light weight nano composite for aero-crafts, *International Journal of Science and Research (IJSR)*, 4(5) (2015) 1892-1895.
- [6] D. Ni, J. Wang, Z. Zhou, Z. Ma, Fabrication and mechanical properties of bulk NiTi/Al composites prepared by friction stir processing, *Journal of Alloys and Compounds*, 586 (2014) 368-374.
- [7] R.S. Mishra, Z. Ma, I. Charit, Friction stir processing: a novel technique for fabrication of surface composite, *Materials Science and Engineering: A*, 341(1-2) (2003) 307-310.
- [8] M. Raft, T. Mahmoud, H. Zakaria, T. Khalifa, Microstructural, mechanical and wear behavior of A390/graphite and A390/Al₂O₃ surface composites fabricated using FSP, *Materials Science and Engineering: A*, 528(18) (2011) 5741-5746.
- [9] R. Miranda, T.G. Santos, J. Gandra, N. Lopes, R. Silva, Reinforcement strategies for producing functionally graded materials by friction stir processing in aluminium alloys, *Journal of Materials Processing Technology*, 213(9) (2013) 1609-1615.
- [10] S. Sahraeinejad, H. Izadi, M. Haghshenas, A. Gerlich, Fabrication of metal matrix composites by friction stir processing with different particles and processing parameters, *Materials Science and Engineering: A*, 626(1) (2015) 505-513.
- [11] A. Devaraju, A. Kumar, B. Kotiveerachari, Influence of rotational speed and reinforcements on wear and mechanical properties of aluminum hybrid composites via friction stir processing, *Materials & Design*, 45 (2013) 576-585.
- [12] H. Eskandari, R. Taheri, F. Khodabakhshi, Friction-stir processing of an AA8026-TiB₂-Al₂O₃ hybrid nanocomposite: Microstructural developments and mechanical properties, *Materials Science and Engineering: A*, 660 (2016) 84-96.
- [13] E.R. Mahmoud, M. Takahashi, T. Shibyanagi, K. Ikeuchi, Wear characteristics of surface-hybrid-MMCs layer fabricated on aluminum plate by friction stir processing, *Wear*, 268(9-10) (2010) 1111-1121.
- [14] J. Mohamadigangaraj, S. Nourouzi, H.J. Aval, Statistical modelling and optimization of friction stir processing of A390-10 wt% SiC compo-cast composites, *Measurement*, 165 (2020) 108166.
- [15] G.S. Raheja, S. Singh, C. Prakash, Development of hybrid Gr/SiC reinforced AMCs through friction stir processing, *Materials Today: Proceedings*, (2020).
- [16] A. Sharma, V.M. Sharma, P. Jinu, A comparative study on microstructural evolution and surface properties of graphene/CNT reinforced Al6061– SiC hybrid surface composite fabricated via friction stir processing, *Transactions of Nonferrous Metals Society of China*, 29(10) (2019) 2005-2026.
- [17] M.S. Prabhu, A.E. Perumal, S. Arulvel, Development of multi-pass processed AA6082/SiCp surface composite using friction stir processing and its mechanical and tribology characterization, *Surface and Coatings Technology*, (2020) 125900.
- [18] V.K.S. Jain, K. Yazar, S. Muthukumar, Development and characterization of Al5083-CNTs/SiC composites via friction stir processing, *Journal of Alloys and Compounds*, 798(1) (2019) 82-92.
- [19] A. Mertens, A. Simar, H.-M. Montrieux, J. Halleux, F. Delannay, J. Lecomte-Beckers, Friction stir processing of magnesium matrix composites reinforced with carbon fibres: influence of the matrix characteristics and of the processing parameters on microstructural developments, in: *Proceedings of the 9th International Conference on Magnesium Alloys and their Applications*, 2012, pp. 845-850.
- [20] F. Akhlaghi, A. Lajevardi, H. Maghanaki, Effects of casting temperature on the microstructure and wear resistance of compocast A356/SiCp composites: a comparison between SS and SL routes, *Journal of Materials Processing Technology*, 155 (2004) 1874-1880.
- [21] K. Nakata, Y. Kim, H. Fujii, T. Tsumura, T. Komazaki, Improvement of mechanical properties of aluminum die casting alloy by multi-pass friction stir processing, *Materials Science and Engineering: A*, 437(2) (2006) 274-280.
- [22] J.A. Hamed, Effect of welding heat input and post-weld aging time on microstructure and mechanical properties in dissimilar friction stir welded AA7075–AA5086, *Transactions of Nonferrous Metals Society of China*, 27(8) (2017) 1707-1715.
- [23] T. Hirata, T. Oguri, H. Hagino, T. Tanaka, S.W. Chung, Y. Takigawa, K. Higashi, Influence of friction stir welding parameters on grain size and formability in 5083 aluminum alloy, *Materials Science and Engineering: A*, 456(1-2) (2007) 344-349.
- [24] V. Balasubramanian, Relationship between base metal properties and friction stir welding process parameters, *Materials Science and Engineering: A*, 480(1-2) (2008) 397-403.
- [25] K. Elangovan, V. Balasubramanian, Influences of tool pin profile and tool shoulder diameter on the formation of friction stir processing zone in AA6061 aluminium alloy, *Materials & design*, 29(2) (2008) 362-373.
- [26] P. Kah, R. Rajan, J. Martikainen, R. Suoranta, Investigation of weld defects in friction-stir welding and fusion welding of aluminium alloys, *International Journal of Mechanical and Materials Engineering*, 10(1)

- (2015) 26.
- [27] Z. Chen, T. Pasang, Y. Qi, Shear flow and formation of Nugget zone during friction stir welding of aluminium alloy 5083-O, *Materials Science and Engineering: A*, 474(1-2) (2008) 312-316.
- [28] Z. Ma, Friction stir processing technology: a review, *Metallurgical and materials Transactions A*, 39(3) (2008) 642-658.
- [29] W. Wang, Q.-y. Shi, P. Liu, H.-k. Li, T. Li, A novel way to produce bulk SiCp reinforced aluminum metal matrix composites by friction stir processing, *Journal of materials processing technology*, 209(4) (2009) 2099-2103.
- [30] M. Barmouz, M.K.B. Givi, J. Seyfi, On the role of processing parameters in producing Cu/SiC metal matrix composites via friction stir processing: investigating microstructure, microhardness, wear and tensile behavior, *Materials characterization*, 62(1) (2011) 108-117.
- [31] H. Liu, Y. Hu, C. Dou, D.P. Sekulic, An effect of the rotation speed on microstructure and mechanical properties of the friction stir welded 2060-T8 Al-Li alloy, *Materials Characterization*, 123 (2017) 9-19.
- [32] M. Dixit, J.W. Newkirk, R.S. Mishra, Properties of friction stir-processed Al 1100-NiTi composite, *Scripta Materialia*, 56(6) (2007) 541-544.
- [33] M. Azizieh, A. Kokabi, P. Abachi, Effect of rotational speed and probe profile on microstructure and hardness of AZ31/Al₂O₃ nanocomposites fabricated by friction stir processing, *Materials & Design*, 32(4) (2011) 2034-2041.
- [34] V. Nardone, K. Prewo, On the strength of discontinuous silicon carbide reinforced aluminum composites, *Scripta Metallurgica*, 20(1) (1986) 43-48.
- [35] L. Dai, Z. Ling, Y. Bai, Size-dependent inelastic behavior of particle-reinforced metal-matrix composites, *Composites Science and Technology*, 61(8) (2001) 1057-1063.
- [36] W. Miller, F. Humphreys, Strengthening mechanisms in particulate metal matrix composites, *Scripta metallurgica et materialia*, 25(1) (1991) 33-38.
- [37] P. Vijayavel, V. Balasubramanian, S. Sundaram, Effect of shoulder diameter to pin diameter (D/d) ratio on tensile strength and ductility of friction stir processed LM25AA-5% SiCp metal matrix composites, *Materials & Design*, 57 (2014) 1-9.
- [38] S. Ahmadifard, N. Shahin, S. Kazemi, A. Heidarpour, A. Shirazi, Fabrication of A5083/SiC surface composite by friction stir processing and its characterization, *Persian Journal of Science and Technology of Composites*, 2(4) (2016) 31-36.
- [39] R. Kraiklang, J. Onwong, C. Santhaweesuk, Multi-Performance Characteristics of AA5052+ 10% SiC Surface Composite by Friction Stir Processing, *Journal of Composites Science*, 4(2) (2020) 36.
- [40] M. Gupta, F. Mohamed, E. Lavernia, T.S. Srivatsan, Microstructural evolution and mechanical properties of SiC/Al₂O₃ particulate-reinforced spray-deposited metal-matrix composites, *Journal of materials science*, 28(8) (1993) 2245-2259.

HOW TO CITE THIS ARTICLE

M. Houshyar, S. Nourouzi, H. Jamshidi Aval, A Novel AA3105-SiC Composite Fabrication Method, *AUT J. Mech. Eng.*, 5(4) (2021) 583-598.

DOI: [10.22060/ajme.2021.19162.5934](https://doi.org/10.22060/ajme.2021.19162.5934)

